Available online at www.sciencedirect.com
ScienceDirect
Composites: Part B 39 (2008) 782–791
composites Part B: engineering
www.elsevier.com/locate/compositesb

Gas permeability of various graphite/epoxy composite laminates for cryogenic storage systems

Sukjoo Choi [1], Bhavani V. Sankar *

Department of Mechanical and Aerospace Engineering, P.O. Box 116250, University of Florida Gainesville, FL 32611, USA

Received 2 July 2007; accepted 27 October 2007
Available online 24 November 2007

Abstract

Experiments were performed to investigate the effect of cryogenic cycling on the gas permeability of various composite laminates for cryogenic storage systems. Textile composites have lower permeability than laminated composites even with increasing number of cryogenic cycles. Nano-particles dispersed in one of the ply-interfaces in tape laminates do not show improvement in permeability. Micrographs of sections of various specimens provide some insight into formation of microcracks, and damage before and after cryogenic cycling. In laminated tape composites microcracks in various layers connect and form an easy path for gas leakage. Composites wherein plies of different orientations are dispersed rather than grouped show excellent performance even after cryogenic cycling. In textile composites the damage is restricted to regions contained by the weave yarns and hence the permeability does not increase significantly with cryo-cycling.
© 2007 Elsevier Ltd. All rights reserved.

Keywords: A. Laminates; C. Fractography; E. Prepreg; Gas permeability

1. Introduction

In order for the next generation of space vehicles to be affordable, it is critically important to achieve a significant reduction in their structural weight thus reducing the cost of launching payloads into space. Typically various gas storage tanks account for about 50% of the dry weight of a space vehicle. Fiber reinforced composite materials can offer significant weight reduction and they are candidate materials for various cryogenic storage systems e.g., the liquid hydrogen (LH2) storage tanks, in the space vehicles. Fiber reinforced composite materials offer many advantages in the design of cryogenic storage tanks such as high specific stiffness and specific strength, and low coefficient of thermal expansion in the fiber direction.

The LH2 storage tanks experience extreme temperatures during refueling operation and also during atmospheric reentry of the space vehicle. The external structural loads combined with the thermal stresses cause microcrack initiation and propagation which could lead to delamination in composite tanks [1]. The cryogenic storage tank requires that the permeability is extremely low, in fact almost impermeable, so that the cryogenic fuel will not leak through the walls of the storage after cryogenic cycling. Therefore, the gas permeability of the material is a critical factor for effective and reliable performance.

The phenomenon of cryogenic-cycling or simply cryo-cycling in which the composite structure is subjected to room temperature and cryogenic temperature alternately, can lead to progressive damage. In fiber reinforced composites, thermal stresses develop at cryogenic temperature, which causes microcrack initiation and propagation. Thermal stresses develop because of the difference in thermal expansion of the fiber and matrix materials at microscale, and also due to the difference in thermal expansion of adjacent layers of the laminate at macro-scale [2]. When the

* Corresponding author. Tel.: +1 352 392 6749; fax: +1 352 392 7303.
E-mail address: sankar@ufl.edu (B.V. Sankar).
[1] Present address: Department of Aerospace Engineering, Texas A&M University, College Station, TX, USA.

1359-8368/$ - see front matter © 2007 Elsevier Ltd. All rights reserved.
doi:10.1016/j.compositesb.2007.10.010

sum of thermal stresses and stresses due to external loads exceeds a critical value for the material system and layup, microcracks develop. When microcracks in the polymer matrix grow, they become transverse cracks, and when a transverse crack reaches the interface between two layers, the crack deflects through the interface and delamination initiates [3]. Combination of microcracks and delaminations provide a pathway for the cryogenic fuel and other gasses to leak through the walls of the storage system.

The purpose of the present study is to investigate the fundamental issue of gas permeability in composite materials. Gas permeability has been predicted using analytical methods and measured experimentally by many researchers. Roy and Benjamin [3] developed an analytical model to estimate the permeability based on the crack opening displacement with a given delamination length, crack density and loading conditions. Stokes [4] performed an experimental investigation to evaluate the permeability of IM7/BMI laminated composites under bi-axial strains. The permeability experimental facility was constructed following the ASTM Standard D-1434 [5] in which the permeability is determined by the pressure difference across the specimen as a function of time for a specific duration. As the strain was gradually applied, the permeability increased initially and then reached a steady-state until the specimen failed. The crack densities in each layer were measured using optical microscopic inspection. The advantage of this test is that it minimizes the error due to ambient pressure differences during the test. However, this experimental method requires a sophisticate pressure transducer with high sensitivity which is capable of detecting infinitesimal pressure change across the specimen accurately.

Kumazawa et al. [6] performed an experimental investigation to measure the gas leakage of fiber reinforced composites under bi-axial strain and thermal load. Through a combination of experimental testing and finite element analysis, the leakage rate as a function of temperature change was determined as the crack density is assumed to be constant.

Grimsley et al. [7] constructed an experimental facility based on ASTM Standard D-1434 [5] to measure permeability of hybrid composites and related films. The volume-flow rate was estimated by measuring the rate of moving distance of a liquid indicator in a glass capillary tube. And, then the gas transmission rate is converted to volume-flow rate using the ideal gas law. The permeance is calculated by the gas transmission rate per upstream pressure. Herring [8] investigated the permeability of thin film polymers after pre-conditioning the samples.

Nettles [9,10] has made a significant contribution in establishing optimal conditions for permeability experiments. The permeability of laminated composites after experiencing impact loads was determined using the volumetric method [10]. Moreover, the study investigated the various testing conditions that influence the permeability results. When the glass capillary tube is mounted either vertically or horizontally, the variation in permeability results was found insignificant. The permeability tests were performed using various types of liquid indicators in the capillary tube, and again the variation in permeability results was found to be insignificant. Also, the length of liquid indicator does not affect the permeability results. However, glass capillary tubes with inner diameter of 0.4 mm underestimated the permeability than capillary tubes with 1.2 mm and 3 mm diameters. This may be due to the fact that very narrow tubes add to the flow resistance and thus indicate a lower apparent permeability. Nettles also investigated the permeability of composite laminates and bonding materials used for feedline components of a space vehicle before and after cryogenic cycles. Glass et al. [11] determined the permeability of core materials for composite sandwich structure when shear loads are applied on the surface. They used Hexcel HRP honeycomb and Dupont Korex honeycomb materials in the sandwich structures.

The purpose of the present experimental study is to measure the gas permeability of composite laminates used for cryogenic storage tank application. Some of the specimens were subjected to cryo-cycling. It is found that the permeability initially increased rapidly with cryo-cycling, but becomes a constant after several cryogenic cycles. Textile (plain woven) composite specimens exhibited lower permeability and also retained the low values after cryogenic cycling compared to laminated composites. Microscopic examination of specimen cross-sections offers some explanation of behavior of various types of laminates.

2. Standard test method for determining gas permeability

The permeability is defined by the amount of gas that passes through a given material of unit area and unit thickness under unit pressure gradient in unit time. The SI unit of the permeability is mol/s/m/Pa. The standard test method for determining gas permeability is documented in ASTM D14382 (Re-approved in 1997) "Standard Test Method for Determining Gas Permeability Characteristic of Plastic Film and Sheeting [5]". The permeability can be measured by two experimental methods, monometric determination method and volumetric determination methods. The experimental setup for the monometric determination method is shown in Fig. 1 [4,5]. The lower pressure chamber beneath the specimen in Fig. 1 is initially vacuumed and the transmission of the gas through the test specimen is indicated by an increase in pressure. The permeability can also be measured using volumetric determination as shown in Fig. 2 [5]. The lower pressure chamber is exposed to atmospheric pressure and the transmission of the gas through the test specimen is indicated by a change in volume. The gas volume-flow rate is measured by recording the rise of liquid indicator in a capillary tube per unit time. The gas transmission rate (GTR) is calculated using the ideal gas law. The permeance is determined as the gas transmission rate per pressure differential across the specimen. And, then the permeability is determined by multiplying permeance by the specimen thickness.

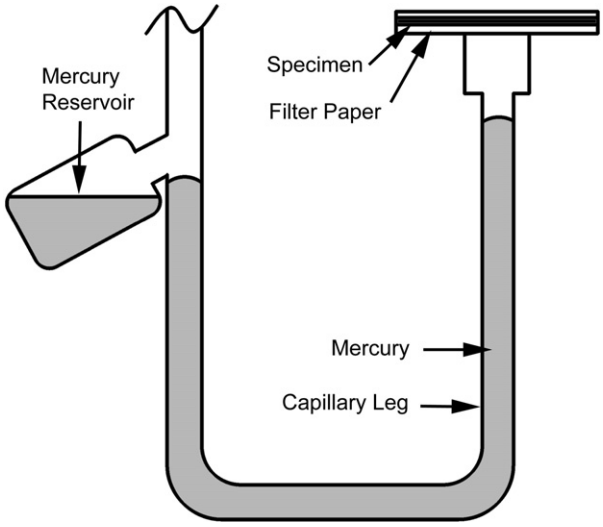

Fig. 1. Permeability experimental setup for monometric determination method [4].

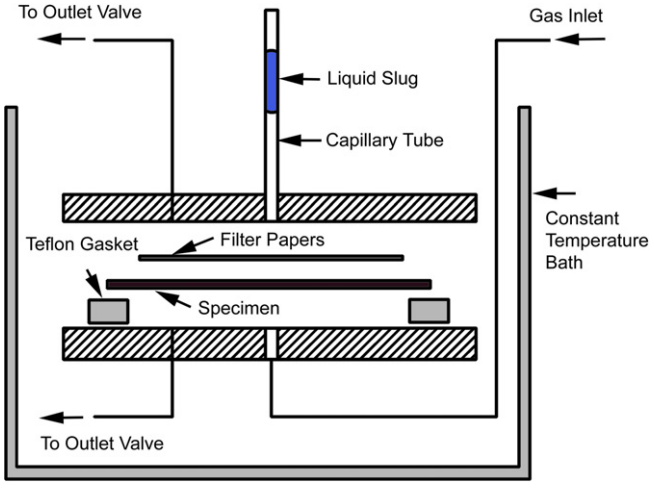

Fig. 2. Permeability experimental setup for volumetric determination method [4].

The monometric determination method was not considered for this study since the mercury compound used in the experiments requires special safety and handling procedures. Therefore, the permeability facility was constructed based on the volumetric determination method as shown in Fig. 2 [5].

3. Permeability apparatus

The permeability experimental apparatus basically consists of two chambers between which the specimen is placed as shown in Fig. 3. The permeant gas is pressurized in the upstream chamber. The gas permeates through one side of the specimen and escapes out of the other side. The escaped gas is collected in the downstream chamber and flows into a glass capillary tube. The amount of gas escaping per unit time is measured. The permeance is determined by gas transmission rate and the pressure differential across the specimen. The permeability $\overline{P}$ is defined by the product of permeance P and the specimen thickness h.

The gauge pressure of the gas in the upper upstream chamber is measured using a pressure transducer (P-303A from the Omega Engineering Inc.). The ambient pressure is measured by a barometric sensor (2113A from the Pasco Scientific). A precision pressure regulator provides constant gas pressure to the upstream chamber. The ambient temperature is measured using a glass capillary thermometer.

The specimens are mounted horizontally between the upstream and downstream chambers and clamped firmly by applying a compressive load (approximately 300 lbs) as shown in Fig. 4. The specimen is sealed with a gasket and an O-Ring (38 mm inner diameter). A force gauge mounted at the top measures the compressive load to ensure that the same amount of compressive load is applied on the specimens for every test. The compressive load should be enough to prevent gas leakage, but should not damage the specimen. The upstream chamber has an inlet vent and an outlet vent. The inlet vent allows the gas flow into the upstream chamber and the outlet vents is used to purge the test gas to atmosphere (see Fig. 4). The downstream chamber has two outlet vents. One is used to purge the test gas to atmosphere and the other allows the gas flow to the glass capillary tube for measurements. The sensitivity of permeability measurement can be improved by increasing the gas transmitting area of a specimen.

The glass capillary tube is mounted on a rigid aluminum base horizontally to minimize the gravity effect on the capillary indicator and for easy reading of the scale marks on the capillary tube. Nettles [9] found that there was no significant difference in the volumetric flow rate when the capillary tube is placed vertically or slanted. The inner diameter of the glass capillary tube is 1.05 mm and the length is 100 mm. A magnifying glass is used to read the scale marks at the top of the meniscus of the liquid indicator.

The liquid indicator in the glass capillary tube is used to measure the rate of rise of the liquid indicator. The rate is used to calculate the volume-flow rate of the escaped gas across the specimen. Nettles [9] investigated the effects on the volume-flow rates by using various types of liquid. The volume-flow rates obtained using water; alcohol and alcohol with PhotoFlo® were not significantly different. In this study methyl alcohol is chosen as the liquid indicator since alcohol has low viscosity and density. The methyl alcohol is colored with a blue dye to obtain precise readings on the scale marks.

The primary objective of this investigation is to study the hydrogen permeability of laminated composites. However, hydrogen gas is highly flammable and explosive when it mixes with air, and it needed to be handled with extreme care during the test. Hence, other permeate gases were considered as a substitute for the hydrogen gas. The molecular

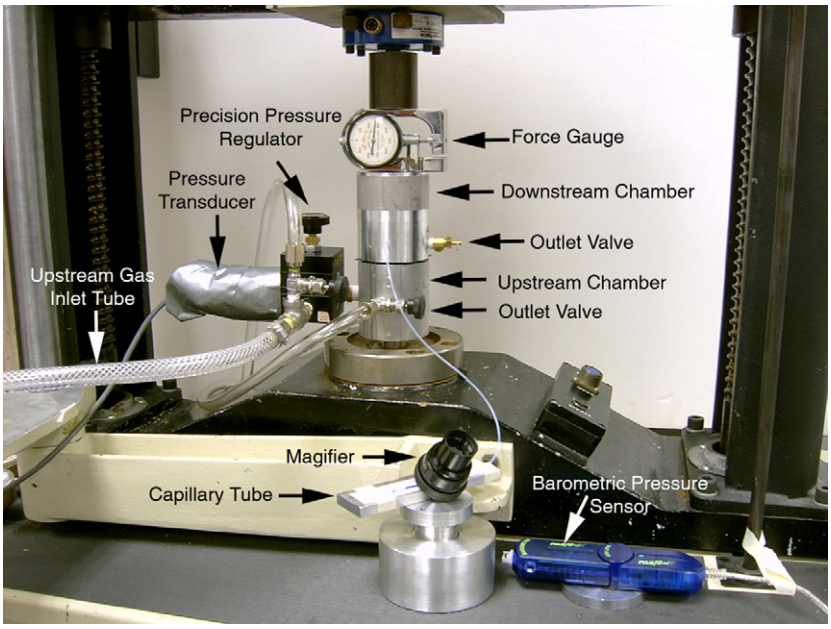

Fig. 3. Permeability testing apparatus.

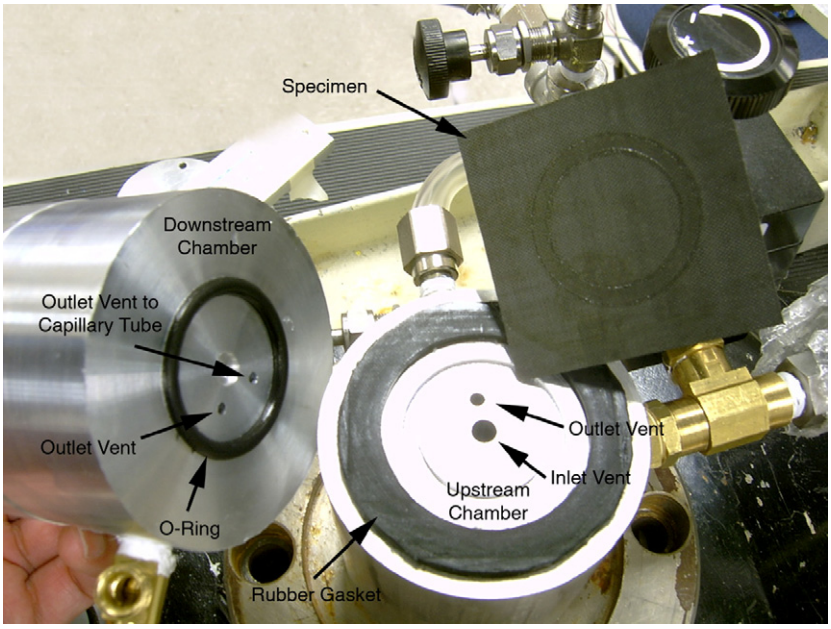

Fig. 4. Specimen installation between upstream and downstream chambers.

Table 1
Molecular diameter of various gases from CRC Handbook of Chemistry and Physics, 54th Edition [8]

Type of gas	From Viscosity	Molecular diameter (cm)	
		From van der Waal's equation	From heat conductivity
Helium	1.9×10^{-8}	2.6×10^{-8}	2.3×10^{-8}
Hydrogen	2.4×10^{-8}	2.3×10^{-8}	2.3×10^{-8}
Nitrogen	3.1×10^{-8}	3.1×10^{-8}	3.5×10^{-8}

diameter of various gases is listed in Table 1 [9]. To choose a permeate gas, the molecular diameter determined from viscosity measurement is mainly considered since the permeability is related with the volumetric flow rate directly. Since helium has the smallest molecular diameter, its apparent permeability is higher than that for other gases [8], and it will yield a conservative value for permeability. Therefore, in this study, helium was chosen as the permeate gas instead of hydrogen.

Table 2
Description of composite specimens

Specimen	Material system	Stacking sequence	Thickness (mm)
C1	Graphite/epoxy laminate	$[0/90/0/90/0/90]_S$	1.52
C2	Graphite/epoxy laminate	$[0_2/90_2/0_2]_T$	0.787
C3	Graphite/epoxy laminate	$[0/90/0_2/90/0]_T$	0.914
C5	Graphite/epoxy laminate	$[0/90_2/0]_T$	0.533
T1	Plain weave textile (SP Systems SE-84)	4 layers	0.686
N1	Graphite/epoxy laminate with nano-particles (NP)	$[0/90/NP/90/0]_T$	0.483

4. Specimen description

The permeability tests were performed with various composite material systems. The details of specimens are described in Table 2. The specimens C1, C2 and C3 are various graphite/epoxy composite laminates. The specimen T1 is a textile composite. The specimen N1 is a laminated composite embedded with 36 nm aluminum oxide (Al_2O_3–alumina) nano-particles. The aluminum oxide was dissolved in alcohol and the compound was applied on a surface on a laminated prepreg using a paint brush.

The graphite/epoxy prepregs were cured in an autoclave and machined by a diamond saw to obtain 3 × 3-inch specimens. The machining was performed at low speed to avoid fiber shattering. The surface was cleaned with acetone and prepared carefully to avoid contamination or damages on the surface of the specimen during machining and subsequent handling.

The specimens were subjected to cryogenic cycling at specified number of times, representing multiple refueling process of a space vehicle. A single cryogenic cycle consisted of cooling down from room temperature to cryogenic temperature and then warming up to room temperature. Initially, specimens were placed at room temperature ($T = 300$ K). And, then the specimens completely submerged in an insulated container filled with liquid nitrogen. The specimens stayed in the container for approximately 2 min. When the specimen reached the boiling temperature of liquid nitrogen ($T = 77$ K), the liquid nitrogen boiling disappears gradually. And, then the specimens were taken out of the container and placed at room temperature for approximately 5 min. The cryogenic cycling procedure is repeated for desired number of times.

5. Testing procedure

Before starting the permeability test, a thin coat of silicon grease was applied on the gasket and an O-ring was placed to improve sealing of contact surfaces of the composite specimen. The excessive silicon grease was wiped out to avoid obstructions of the gas on the transmitting surface of the specimen. All outlet valves were opened initially to avoid sudden pressurization of test gas. The specimen was placed horizontally on the gasket of the upstream chamber. And then, the downstream chamber was placed on the top surface of a specimen. The specimen was mounted between the chambers. Both chambers were aligned and mated as close as possible. The specimen was mounted between the chambers and clamped firmly with a compressive force.

The test gas was admitted to the upstream chamber by opening the gas release valve of the gas tank. While all outlet valves remained opened, the test gas was filled in the upstream chamber and ventilated though the outlet vent to atmosphere. Any residual air in the upstream chamber was purged for about a minute. The outlet valve on the upstream chamber was closed and the test gas was allowed to permeate across the specimen for a sufficient time to purge any residual air in the downstream chamber. At this time, only test gas filled the chambers. When the outlet valve of the upstream chamber was closed, the upstream pressure increased slowly. It is possible that the applied upstream pressure on the specimen causes the specimen deflection and initiates microcracking. However, a finite element analysis of the specimen and the fixture [12] showed that the deflections were not significant enough to affect the permeability. The upstream pressure can be adjusted by controlling the pressure regulator. Sufficient time was allowed for attaining steady-state of moving rate of the liquid indicator before the readings were taken. The distance of rise of the liquid indicator was measured while the ambient pressure was continuously recorded.

6. Calculations

The volumetric methodology is used to calculate the permeability by measuring gas volume transmitted through the specimen. The rate of rise of the liquid indicator is used to calculate the volume-flow rate V_r as follows:

$$V_r = \text{slope} \times a_c \tag{1}$$

where a_c is the cross-sectional area of a capillary tube and the slope is the rate of rise of the liquid indicator in the capillary tube in m/s unit. The gas transmission rate (GTR) is calculated using the ideal gas law as:

$$\text{GTR} = \frac{p_o \cdot V_r}{ART} \tag{2}$$

where p_o is ambient pressure, A is transmitting area of the specimen, R is the universal gas constant (8.3143×10^3 L Pa/{mol K}) and T is ambient temperature in degree Kelvin. The permeance P is defined by the ratio between

the gas transmission rate and pressure differential across the thickness of the specimen, and it is calculated as:

$$P = \frac{\mathrm{GTR}}{p - p_o} \tag{3}$$

where p is the upstream pressure. The S.I. unit of permeance is [mol/(m^2 s Pa)].

According to the standard test method, the permeability $\overline{P}$ is defined by the product of permeance P and the specimen thickness h. Although the permeability is meaningful only for homogeneous materials [5], the same methodology is used for laminated composites in this study. Hence the permeability should be considered as the average for the laminate rather than the material property of the composite material system.

7. Calibration

The position of capillary indicator is very sensitive to even small variations of testing conditions such as ambient pressure and temperatures caused by closing doors or air-conditioning system in the laboratory. For example, during one test, the variation of the ambient pressure was approximately 0.3% for a 13-h period (Fig. 5). For the permeability calculation, the ambient pressure is assumed to be constant. However, for a long time period, the variation is large enough to cause error in measuring the rate of rise of the capillary indicator. The moving distance needs to be calibrated to compensate for error due to the variation of ambient pressure.

The error correction factor due to the variation of ambient pressure was calculated by performing the permeability test without applying the upstream pressure. An aluminum plate is used for the test to ensure that there is no gas permeation to the downstream chamber. Since there was not much variation in the ambient temperature, only ambient pressure causes changes in the position of the capillary indicator. After the outlet valve of the downstream chamber was closed, the displaced position of the capillary indicator and ambient pressure were measured simultaneously as shown in Fig. 6.

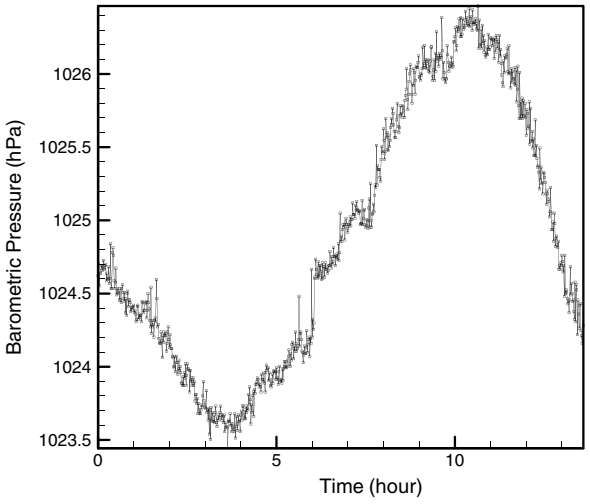

Fig. 5. Variation of ambient pressure for 13 h at test conditions.

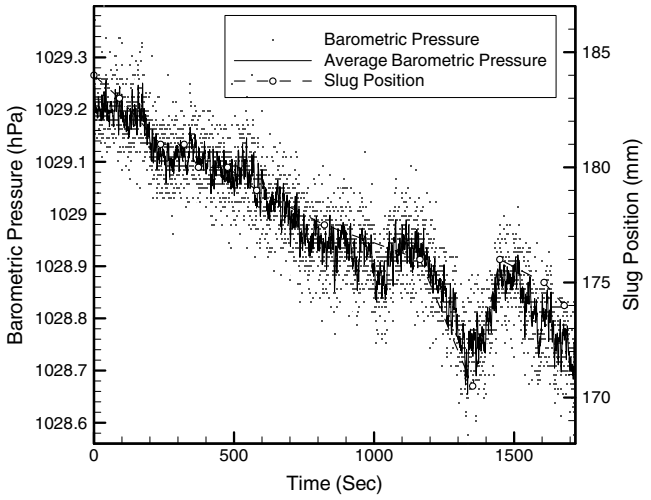

Fig. 6. Variation of barometric pressure and indicator position as a function of time.

The correction factor k is calculated by $k = \Delta h/\Delta p$ where h is the moving distance of the capillary indicator and p is the ambient pressure. The average correction factor is found to be 0.21 mm/Pa. Therefore, the corrected moving distance of the capillary indicator is calculated as follows:

$$h_{\mathrm{corrected}} = h_{\mathrm{actual}} + k \cdot \Delta p \tag{4}$$

where Δp is differential of ambient pressure between the beginning and end of the test.

8. Permeability test results

The permeability tests were performed with various composite material systems at room temperature. The permeability was measured at six different levels of upstream pressure. The average permeance P and average permeability $\overline{P}$ are tabulated in Table 3 for laminated composites, the results for textile composites are in Table 4 and the results for laminated composites embedded with nano-particles in Table 5.

The test results show that the permeability increases as the number of cryogenic cycles increases (see Fig. 7). The permeability increased rapidly and becomes constant with further increase of cryogenic cycles. For specimens C2 ($[0_2/90_2/0_2]_T$) and C3 ($[0/90/0_2/90/0]_T$), which have approximately same thickness, the permeability of the specimen C3 was lower since the specimen C3 has the 0° and 90° plies dispersed and not grouped together compared to the specimen C2. The four-layer plain weave textile specimen T1 maintained constant permeability with the increase of cryogenic cycles. The textile composites produced lower permeability than the laminated composites (C1, C2 C3 and C5). The specimen N1 has the same stacking sequence as spec-

Table 3
Permeability of laminated composites before and after cryogenic cycling

Specimen	Number of cryogenic cycles	Permeance, P (mol/s/m^2/Pa)	Permeability, $\overline{P}$ (mol/s/m/Pa)	Logarithm of $\overline{P}$
C1$[0/90/0/90/0/90]_S$	0	5.60×10^{-18}	8.54×10^{-21}	−20.1
	1	1.52×10^{-17}	2.32×10^{-20}	−19.6
	5	2.39×10^{-17}	3.65×10^{-20}	−19.4
	10	2.39×10^{-17}	3.65×10^{-20}	−19.4
	20	2.11×10^{-17}	3.22×10^{-20}	−19.5
C2$[0_2/90_2/0_2]_T$	0	7.02×10^{-18}	1.07×10^{-20}	−20.0
	1	1.06×10^{-17}	1.62×10^{-20}	−19.8
	5	1.47×10^{-15}	2.23×10^{-18}	−17.7
	10	1.42×10^{-15}	2.16×10^{-18}	−17.7
	20	1.49×10^{-15}	2.27×10^{-18}	−17.6
C3$[0/90/0_2/90/0]_T$	0	6.22×10^{-18}	9.48×10^{-21}	−20.0
	1	7.56×10^{-18}	1.15×10^{-20}	−19.9
	5	7.60×10^{-18}	1.16×10^{-20}	−19.9
	10	8.37×10^{-18}	1.28×10^{-20}	−19.9
C5$[0/90_2/0]_T$	0	5.85×10^{-18}	8.92×10^{-21}	−20.0
	1	9.52×10^{-16}	1.45×10^{-18}	−17.8
	5	8.67×10^{-16}	1.32×10^{-18}	−17.9
	20	8.81×10^{-16}	1.34×10^{-18}	−17.9

Table 4
Permeability of textile composites (Specimen T1) before and after cryogenic cycling

Number of cryo-cycles	Permeance, P (mol/s/m^2/Pa)	Permeability, $\overline{P}$ (mol/s/m/Pa)	Logarithm of $\overline{P}$
0	4.79×10^{-18}	7.30×10^{-21}	−20.1
1	6.77×10^{-18}	1.03×10^{-20}	−20.0
5	8.41×10^{-18}	1.28×10^{-20}	−19.9
20	8.75×10^{-18}	1.33×10^{-20}	−19.9

Table 5
Permeability of laminated composites embedded with nano-particles (Specimen N1, $[0/90/NP/90/0]_T$) after various numbers of cryogenic cycles

Number of cryo-cycles	Permeance, P (mol/s/m^2/Pa)	Permeability, $\overline{P}$ (mol/s/m/Pa)	Logarithm of $\overline{P}$
0	6.82×10^{-18}	1.04×10^{-20}	−20.0
1	2.72×10^{-15}	4.15×10^{-18}	−17.4
5	1.30×10^{-14}	1.98×10^{-17}	−16.7
20	9.83×10^{-15}	1.50×10^{-17}	−16.8

imen C5 ($[0/90_2/0]_T$), but it has nano-particles dispersed between two 90° layers. Before cryogenic cycling, the permeabilities of the specimens N1 and C5 were approximately the same. However, as the number of cryogenic cycles increased, the permeability of the specimen N1 became higher. Dispersion of nano-particles at one of the ply interfaces did not reduce the permeability of the laminated composite.

9. Optical microscopic analysis

Results discussed in the preceding section indicate that the permeability increases as the composite specimen underwent more cryogenic cycles. As the crack density increases, gas flow becomes easier though the specimen. It is conjectured that cryo-cycling, in general, increases the number of microcracks in the specimens and hence make it easier for the gas to permeate. In order to verify this behavior, optical micrographic studies were performed.

The specimens were cut through the center using a diamond saw. A LECO grinder/polisher was used for the sample preparation process. The cut surface was ground with 600-grit sand paper under wet condition for 30 s. The fine grinding was performed with the 1000-grit and 1500-grit papers for 30 s. The surface of the edge was polished with the 58 μm aluminum oxide powder (Al_2O_3-alumina) dissolved in distilled water. The purpose of the lubricant is

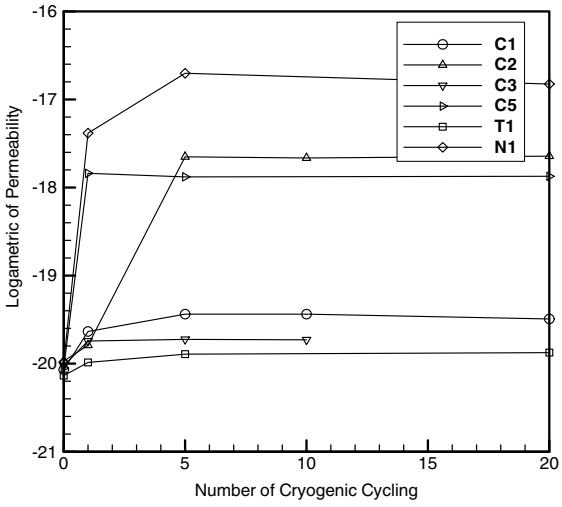

Fig. 7. Logarithm of the permeability for composite specimens with increase of cryogenic cycles. Laminated tape composite specimens C1 and C3 have the 0° and 90° plies dispersed and hence seem to have lower permeability after cryogenic cycling.

to both dissipate the heat from polishing and to act as a carrier for the abrasive materials. The ultrasonic cleaner was used to remove any abrasive particles and contaminants on the polished surface of a specimen. The optical analysis was conducted with a NIKON EPIPOT microscope.

The laminated composite specimen C2 and the textile composite specimen T1 were subjected to optical inspection

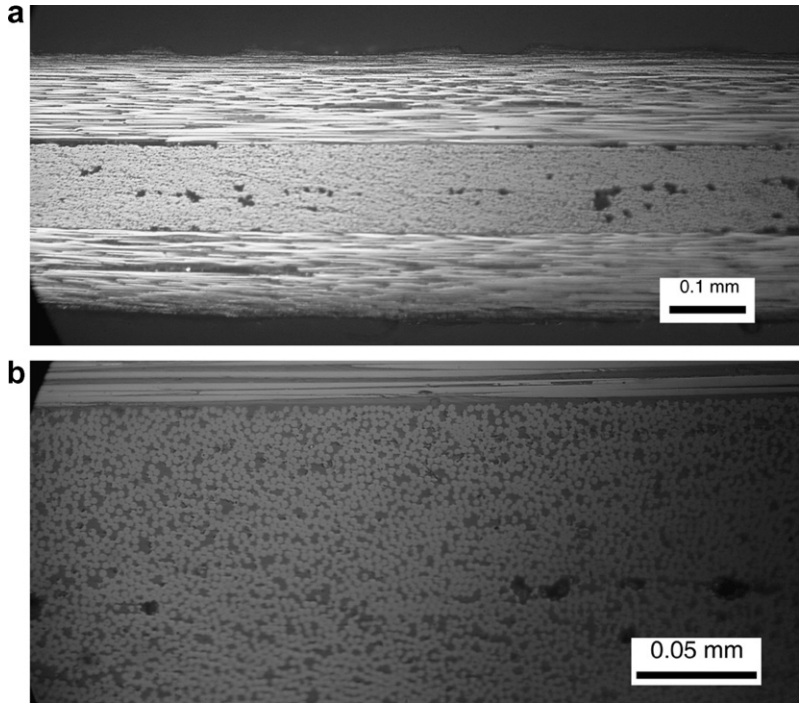

Fig. 8. Cross-sectional view of the graphite/epoxy composite specimen C2 before cryogenic cycling: (a) 10× magnification; (b) 40× magnification.

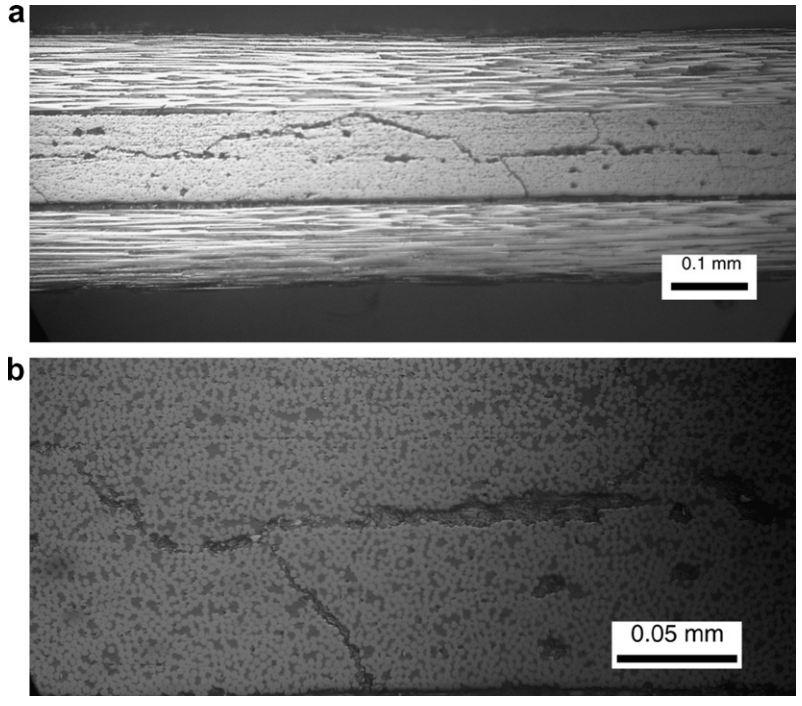

Fig. 9. Microcrack propagation in the graphite/epoxy composite specimen C2 after 5 times of cryogenic cycles: (a) 10× magnification; (b) 40× magnification.

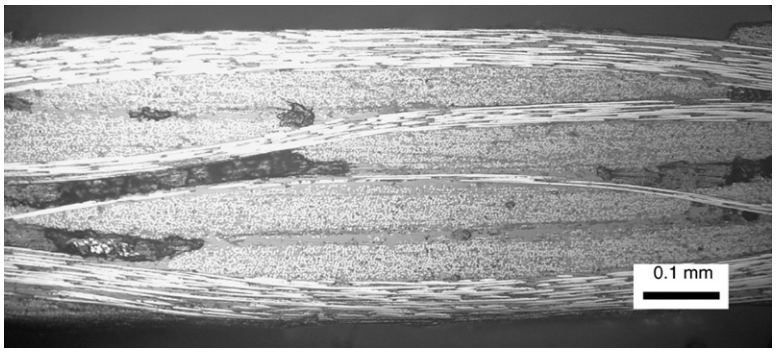

Fig. 10. Cross-sectional view of the woven composite specimen T1 before cryogenic cycling, 10× magnification.

since these specimens have same thickness but different microstructures. The specimen details are described in Table 2. The microscopic images of the specimens were compared before and after cryogenic cycling.

For the graphite/epoxy specimen C2 before cryogenic cycling, no microcrack propagation is observed (see Fig. 8). Some voids were observed in the middle of the 90° layers and between the 0° and the 90° layers. The voids were probably formed by trapped air bubbles during composite fabrication in the autoclave. After cryogenic cycling, microcracks were observed in the 90° layer of C2 (see Fig. 9). No fiber breaks were observed in the 0° layer since the thermal stresses were not large enough [13]. The delaminations propagated along the middle of the 90° layer where some voids were found. The transverse cracks branched into ply delaminations. Since the gas can be transmitted through the transverse cracks across the specimen, the permeability increased after cryogenic cycling.

For the textile composite specimen T1, no microcracks were observed before cryogenic cycling as shown in Fig. 10. Voids were observed at the location where two yarns intersect. After the textile composite specimen T1 underwent cryogenic cycles, microcracks were observed in the 90° yarn as shown in Fig. 11. The microcracks propagated in the in-plane direction of the specimen and they seem to be contained within the pocket formed between the textile yarns. Since transverse cracks did not propagate, the permeability of textile composites was almost the same before and after cryogenic cycling.

The transverse cracks and delaminations provide the leakage path through composite laminates and thus directly relate to the permeability. In the textile composite

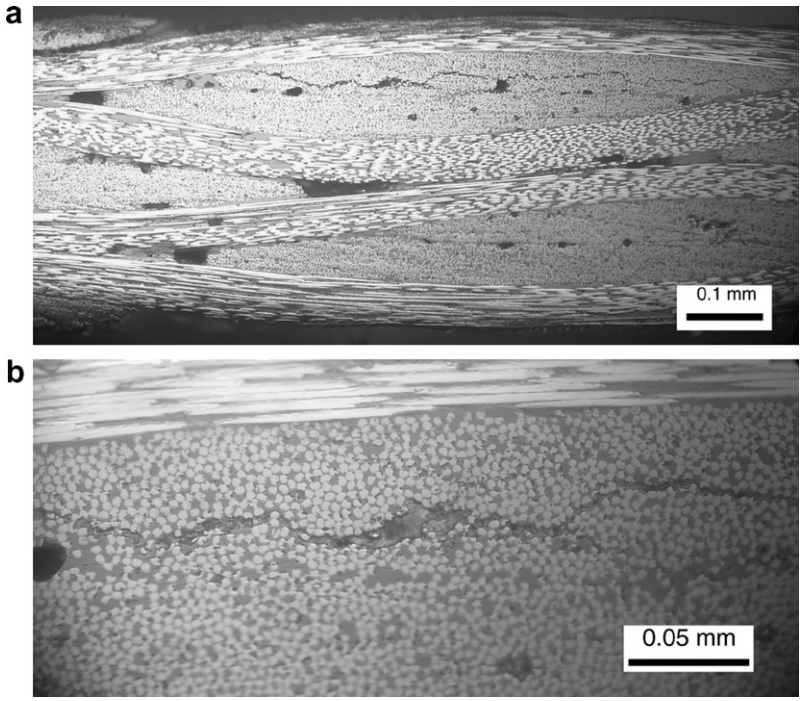

Fig. 11. Microcrack propagation in the woven composite specimen T1 after 5 times of cryogenic cycles: (a) 10× magnification; (b) 40× magnification.

specimen, the transverse cracks propagation was not observed, which resulted in low permeability even after cryogenic cycling.

10. Summary

An experimental study was conducted to measure the gas permeability of various composite material systems and to study the effect of cryogenic cycling on the permeability. The permeability test facility was constructed following the standard test method documented in ASTM D14382 (Re-approved 1997). The permeability test was conducted at room temperature using gaseous helium. A calibration was performed to compensate for the ambient pressure changes during the test. The permeability of laminated composites was found to increase anywhere between 3% to 12% after cryogenic cycling. The permeability of thin laminated specimens increased significantly after cryogenic cycling. The textile composite specimen has lower permeability than laminated specimens, and the increase of permeability is small (about 1%) with the increase in cryogenic cycles. Cross-ply laminates, wherein the plies are dispersed well (not grouped together) exhibit less permeability after cryogenic cycling. Dispersing nano alumina particles at the interface of two plies did not show any reduction in permeability. Further studies are needed to investigate the effects of nano-particles. Photomicrographs of several specimen cross-sections were analyzed. In the case of textile composites, microcracks develop during cryogenic cycling, but they do not connect and hence do not contribute to increase in permeability.

Acknowledgements

The authors gratefully acknowledge the technical and financial support of NASA Glenn Research Center (NAG3-2750) and NASA Kennedy Space Center under the Hydrogen Research and Education program. Partial support was provided by the CUIP (URETI) Program sponsored by NASA under NCC3-994, managed by NASA Glenn Research Center.

References

[1] Rivers HK. Cyclic cryogenic thermal–mechanical testing of an X-33/RLV liquid oxygen tank concepts, NASA/TM-1999-209560. Langley Research Center, Hampton, Virginia, 1999.
[2] Choi S, Sankar BV. Fracture toughness of a transverse crack in laminated composites at cryogenic conditions. Composite Part B: Eng 2007;38:193–200.
[3] Roy S, Benjamin M. Modeling of permeation and damage in graphite/epoxy laminates for cryogenic fuel storage. Compos Sci Technol 2004;64:2051–65.
[4] Stokes E. Hydrogen permeability of polymer based composite tank material under tetra-axial strain. In: Proceedings of the fifth conference on aerospace materials, processes and environment technology (AMPET), Huntsville, Alabama, September 16–18, 2002. http://www2.southernresearch.org/pdf/tetraaxial_strain.pdf.
[5] ASTM D1434-82 (Re-approved 1992), Standard test method for determining gas permeability characteristics of plastic film and sheeting, ASTM, 1992. p. 203–13.
[6] Kumazawa H, Aoki T, Susuki I. Analysis and experiment of gas leakage through composite laminates for propellant tanks. AIAA J 2003;41(10):2037–44.
[7] Grimsley B, Cano R, Johston N, Loos A, McMahon W. Hybrid composites for LH2 fuel tank structure. In: Proceedings of the 33rd international SAMPE technical conference, NASA Langley Research Center, November 4–8, 2001.
[8] Herring H. Characterization of thin film polymers through dynamic mechanical analysis and permeation, NASA/CR-2003-212422, 2003.
[9] Nettles AT. Permeability testing of impacted composite laminates for use on reusable launch vehicles, NASA/TM-2001-210799, 2001.
[10] Nettles AT. Permeability testing of composite materials and adhesive bonds for the DC-XA composite feedline program, NASA Technical Memorandum 108483, March 1995.
[11] Glass E, Venkat V, Sankaran S. Honeycomb core permeability under mechanical loads, NASA/CR-97-206263, 1997.
[12] VanPelt III, J. Effect of strain on the gas permeability of composite laminates. Master Thesis, University of Florida, Gainesville, Florida, December 2006.
[13] Choi S, Sankar BV. Micromechanics method to predict micro stresses in fiber composite materials. J Compos Mater 2006;40(12):1077–91.